



Nanosized NiS₂-Photosensitized TiO₂ Coating on Multi-walled Carbon Nanotubes with Higher Visible Light Photocatalytic Activity†

LEI ZHU, ZE-DA MENG, CHONG-YEON PARK, JONG-GEUN CHOI, TRISHA GHOSH and WON-CHUN OH*

Department of Advanced Materials Science & Engineering, Hanseo University, Seosan-si, Chungnam-do, 356-706, South Korea

*Corresponding author: Fax: +82 41 6883352; Tel: +82 41 6601337; E-mail: wc_oh@hanseo.ac.kr

AJC-11352

A simple synthesis route to nanoscale NiS₂-CNT/TiO₂ photocatalyst by a sol-gel method was developed and the visible light photocatalytic activity of the obtained samples for the degradation of methyl orange was studied. The prepared photocatalysts were characterized by XRD, EDX SEM, TEM and BET. For as prepared samples, anatase titanium dioxide and nickel sulfide particles were uniformly deposited on the surface of multi-walled carbon nanotubes. The visible light photocatalytic properties were successfully demonstrated by decoloration of methyl orange. The results indicate that the addition of an appropriate amount of multi-walled carbon nanotubes as supports for TiO₂ and NiS₂ efficiently inhibit the agglomeration of NiS₂/TiO₂ and extended the light absorption spectrum into the visible region due to the excellent photoelectric characteristics of semiconductor NiS₂.

Key Words: NiS₂, Multi-walled carbon nanotubes, TiO₂, Visible-light photocatalysis, Methyl orange.

INTRODUCTION

Titanium dioxide (TiO₂) has advantages over other photocatalysts, such as high activity, good stability, low cost and little harmness to humans. However, the main drawback of TiO₂ is its relatively large band-gap (anatase: 3.2 eV, rutile: 3.0 eV). As a consequence, TiO₂ shows photocatalytic activity only in the near ultraviolet region and can harvest only a small fraction (< 5 %) of incident solar irradiation¹. Therefore, modifying TiO₂ photocatalysts to enhance light absorption and photocatalytic activity under visible light irradiation becomes the main research direction in recent years. To improve the response of TiO₂ to visible light, transition metal² or non-metal atom³ doped TiO₂ or metal complex⁴ sensitized TiO₂ have been developed. Alternative approach for achieving this objective is to coupling of TiO₂ by using a narrow band gap semiconductor with a higher conduction band (CB) than that of TiO₂. In this sensitized TiO₂, charge injection from the conduction band of the narrowband gap semiconductor to that of TiO₂ can lead to efficient and longer charge separation by minimizing the electron-hole recombination.

The present work focused on the coupled semiconductors in nanoscale. It has been reported that the development of the coupled semiconductors with nanometer sizes is one of the effective approach to prepare the photocatalytic materials that

can utilize the sunlight effectively. In addition, these coupled semiconductors including MS/TiO₂ (M = Pb, Zn, Cd) also exhibit fine optical properties (absorption and photoluminescence) compared with the corresponding bulk ones due to the quantum confinement effects⁵. Nickel sulfide, as an important inorganic functional material, has attracted much attention because of practical applications, such as metal-insulator, paramagnetic-antiferromagnetic (PM-AFM) phase-changing material, magnetic refrigeration, magnetic resonance imaging and microwave absorption material⁶. However, NiS₂/TiO₂ photocatalyst in our studies has some shortcomings. For example, a combined NiS₂ semiconductor can easy to become a recombination center for photo-electron-hole pairs and has a low specific surface area in most cases, which can limit the rate of photodegradation meanwhile there are some dispersion problems due to this nanoparticles are easy to cohere.

To solve the problems, multi-walled carbon nanotubes (MWCNTs) as good support was used in this study due to its unique mechanical, optical and electrical properties that may impact many fields of science and technology. MWCNTs, as a new class of nanomaterials, have been drawn to considerable attention for their applications as catalyst supports owing to their unique electrical properties, high chemical stability and high surface-to-volume ratio. Moreover, MWCNTs have a variety of electronic properties. They may also exhibit metallic

†Presented to The 5th Korea-China International Conference on Multi-Functional Materials and Application.

conductivity as one of the many possible electronic structures. Multi-walled carbon nanotubes have a large electron-storage capacity (one electron for every 32 carbon atoms)⁷, the ability of MWCNTs can promote the electron-transfer reactions at carbon nanotubes modified materials. Thus far, CNTs modified with nanocrystalline semiconductor particles have been proven to be more active owing to their size-dependant nonlinear optical, physical and electronic properties, which make them promising materials with potential application in several fields^{8,9}.

Additionally, doping with non-metallic species¹⁰⁻¹⁵, such as N, C, S, P and halogen atoms also caused the photosensitization of TiO₂ in the visible light region. Among various non-metal modified titania, carbon-containing composites titania has been reported as a kind of promising photocatalyst. Kisch and co-workers^{10,11} reported that carbon containing titania prepared by a modified sol-gel process using different alkoxide precursors was able to photo degrade *p*-chlorophenol under visible light ($\lambda > 400$ nm). Treschev *et al.*¹² found carbon-containing TiO₂ nanoparticles prepared under calcinations at 200 °C exhibited high photocatalytic activity for decoloring of methylene blue and the removal of nitrogen monoxide under visible light illumination. Kang *et al.*¹⁶ synthesized C-doped TiO₂ powders by grinding TiO₂ with ethanol and heating treatment and this C-doped TiO₂ photocatalyst showed a good visible light activity for NO gas decomposition. Chen and co-workers¹⁷ synthesized C-doped TiO₂ micronanosphere and nanotubes *via* a chemical vapour deposition method and they claimed that carbon doping led to lower band gap and higher photocurrent than TiO₂ P₂₅ under visible light irradiation.

Therefore, we combined we combined both advantages of introduced MWCNT and NiS₂ to design an effective NiS₂-CNT/TiO₂ nano-composite photocatalyst for methyl orange (C₁₄H₁₄N₃NaO₃S) decomposition. The intrinsic characteristics of the photocatalysts were studied by X-ray powder diffraction (XRD) and the determination of Brunauer-Emmett-Teller (BET) surface areas. The photocatalytic activity of the as-synthesized samples was evaluated by degradation methyl orange under visible light irradiation.

EXPERIMENTAL

Multi-walled carbon nanotube (95.5 %) powder, containing nanotubes with diameters of 20 nm and lengths up to 5 μ m, was purchased from Carbon Nano-material Technology Co. Ltd., Korea. To oxidize the surface of the MWCNTs, we used *m*-chloroperbenzoic acid (MCPBA) purchased from Acros Organics, New Jersey, USA as an oxidized reagent. Reagent-grade benzene (99.5 %) and ethanol were purchased from Duksan Pure Chemical Co. (Korea) and Daejung Chemical Co. (Korea) and used as received. Titanium(IV) *n*-butoxide (TNB, C₁₆H₃₆O₄Ti) was used as a titanium source. Nickel chloride (NiCl₂) and sodium sulfide 5-hydrate (Na₂S·5H₂O) were used for the preparation of NiS₂ and were supplied by Duksan Pure Chemical Co. Ltd., Korea and Yakuri Pure Chemicals Co. Ltd., Japan, respectively. Analytical grade methyl orange (C₁₄H₁₄N₃NaO₃S) was purchased from Samchun Pure Chemical Co. Ltd., Korea. Titanium oxide nanopowder (TiO₂, < 25 nm, 99.7 %) with anatase structure used as original sample was purchased from Sigma-Aldrich Chemistry, USA.

All chemicals were used without further purification and all experiments were carried out using distilled water.

Chemical oxidation on the nanocarbon surface: *m*-Chloroperbenzoic acid (MCPBA, *ca.* 1 g) was suspended in 80 mL of benzene, followed by addition of MWCNT (*ca.* 40.0 mg), whereupon the mixture was refluxed in air for 6 h. The solvent was then removed through distillation, leaving a dark brown precipitate. The precipitate was then washed with ethyl alcohol and dried at 100 °C.

Preparation of NiS₂-CNT/TiO₂ nanocomposites: MWCNT is very stable against weak acids or bases and needs to be treated with strong acids to introduce active function groups to its surface. *m*-Chloroperbenzoic acid (*ca.* 2 g) was suspended in 80 mL benzene as a solvent. Subsequently, 1 g MWCNTs powder was added to the agent solution and the mixture was treated by magnetic stirring for 6 h at 343 K. Furthermore, the resulting solution was washed continuously with deionized water and ethanol before drying at 363 K.

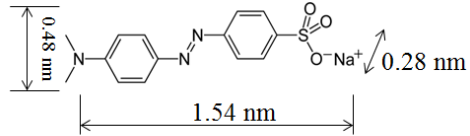
Nickel chloride powder was dissolved in 30 mL of water. After stirring the solution magnetically for 10 min, 0.3 g of oxidized MWCNTs was added to the solution and stirred further for 0.5 h. A Na₂S solution (30 mL) was prepared separately and added dropwise to the solution with constant stirring for 6 h at 343 K. The mixture was transformed to a black green colour. After completion, the black green solution was filtered, washed with distilled water and ethanol and then dried at 353 K. The compound was milled and heat treated at 573 K for 1 h. Finally, a NiS₂/CNT composite was obtained.

To prepare the NiS₂-CNT/TiO₂ composite, a small amount of powdered NiS₂/CNT composite was added to 5 mL of TNB containing 15 mL of benzene. After stirring for 5 h at 343 K, the powder mixtures of NiS₂/CNT reacted with TNB were dried at 353 K for 12 h. Finally, the sample was heated to 623 K for 1 h. Fig. 1 gives the procedure for preparing the NiS₂-CNT/TiO₂ composites. For comparison, CNT/TiO₂ photocatalyst was synthesized using similar procedures except for heating at 773 K for 1 h.

Catalysts characterization: Crystallographic structure of the composites photocatalysts were obtained by XRD (Shimatz XD-D1, Japan) at room temperature with CuK α radiation ($\lambda = 0.154056$ nm) and a graphite monochromator, operated at 40 KV and 30 mA. Transmission electron microscopy (TEM, JEOL, JEM-2010, Japan) with an accelerating voltage of 200 kV was used to examine the size and distribution of the photocatalysts. The EDX spectra were also used for elemental analysis of the samples. The BET surface area of the photocatalysts was determined through nitrogen adsorption at 77 K using a BET analyzer (Monosorb, USA). All the samples were degassed at 623 K before the measurement. The UV-VIS adsorption parameters for dye solution degraded by anatase TiO₂, NiS₂-CNT/TiO₂ composites photocatalysts under visible light irradiation were recorded using a UV-VIS (Optizen Pop Mecasys Co. Ltd., Korea) spectrometer.

Photocatalytic activity test: The photocatalytic activities of samples were evaluated in terms of the degradation of methyl orange (C₁₄H₁₄N₃NaO₃S) decomposition in aqueous solution under visible light illumination. The molecular structure and λ_{max} of organic dyes are shown in Table-1. The

TABLE-1
MOLECULAR STRUCTURE AND ABSORBANCE MAXIMUM (λ_{\max}) OF METHYL ORANGE

Organic dyes	Molecular structure	λ_{\max}
Methylene orange (MO)		465 nm

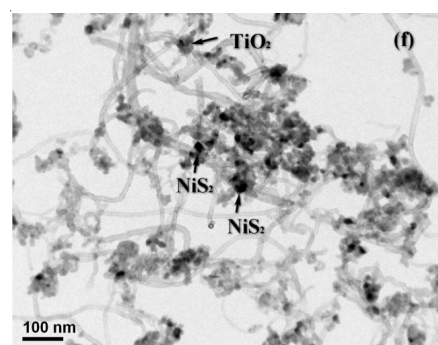
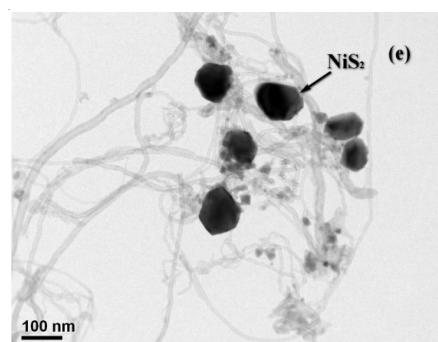
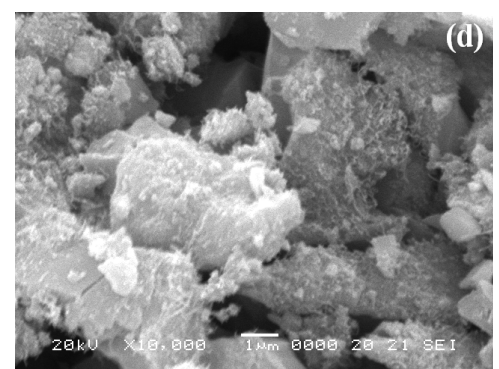
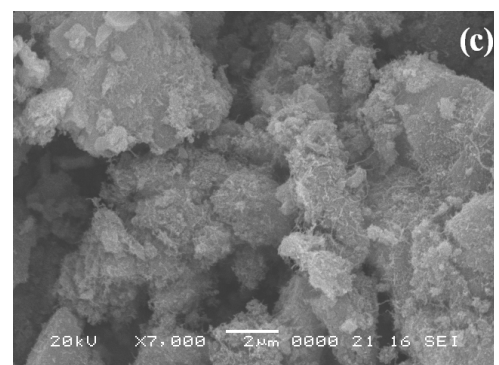
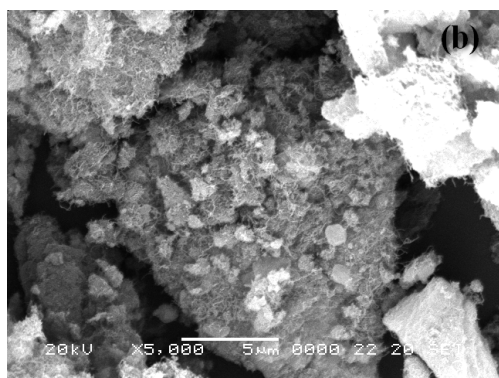
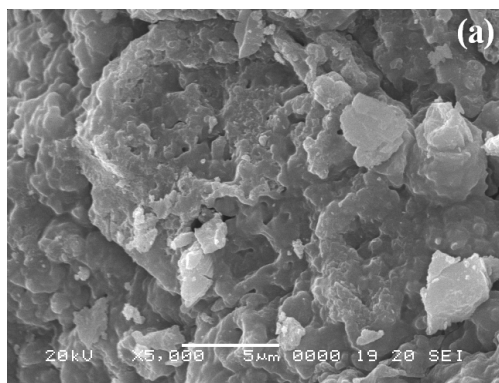


Fig. 1. SEM and TEM micrographs of as-prepared samples: (a) NiS₂, (b,e) NiS₂-CNT, (c) CNT/TiO₂, (d,f) NiS₂-CNT/TiO₂

photodegradation reactions were carried out with a homemade photoreactor. For visible light irradiation, the reaction beaker was located axially and held in a visible lamp (8W, halogen lamp, KLD-08L/P/N, Fawoo Technology, Korea) box. The luminous efficacy of the lamp is 80 mL/W and the wave length is 400 nm to *ca.* 790 nm. The distance between the light and the reaction tube was fixed at 100 mm. The initial concentration of methyl orange (c_0) was 2.0×10^{-5} mol/L. The photocatalyst powder (0.03 g) was dispersed in a 100 mL glass photoreactor containing 100 mL of dye solution. The mixture was stirred for 0.5 h in the dark in order to reach the adsorption-desorption equilibrium. At the given time intervals the sample of 3.5 mL was taken from the mixture and immediately centrifuged to remove the dispersed photocatalysts. The concentration of the clean transparent solution was analyzed by checking the absorbance at 467 nm for methyl orange with the UV-VIS spectrophotometer.

RESULTS AND DISCUSSION

Characterization: The typical micro-surface structures and morphology of the NiS₂ and NiS₂-CNT/TiO₂ composites were characterized by SEM (Fig. 1a-d). For the prepared NiS₂ composite mainly consists of shaped particles with smooth surface and have a high tendency to agglomerate. It can be attributed that when the crystal particle size is very small, it

can easily agglomerate due to the weak forces of the surface. As-prepared NiS₂-CNT/TiO₂ composites exhibit famous properties about the surface nanostructures which were studied in Fig. 1d.

For the obtaining of the surface nanostructures and particle sizes of NiS₂/CNT and NiS₂-CNT/TiO₂ composites were studied by TEM (Fig. 1 e-f). It can be clearly seen that the TiO₂ and NiS₂ particles of 10-20 nm size were regularly and individually distributed on the MWCNTs surface. This indicates that the presence of the MWCNTs can efficiently inhibit the agglomeration of NiS₂/TiO₂ and improve the dispersion of nanoparticles.

The crystal phase structures of as-prepared samples were characterized by X-ray diffraction measurements (Fig. 2). It can be confirmed that the TiO₂ in three as-prepared photocatalysts is anatase-phase. For these two samples, (101), (004), (200), (105), (211) and (204) crystal planes are originated from the anatase TiO₂ phase (JCPDS file, No. 21-1272), while all the peaks can be indexed as a simple cubic lattice with the cell constant $a = 5.678 \text{ \AA}$, which is consistent with the reported data for NiS₂ (JCPDS Card File No. 65-3325)¹⁸. The broadening of the diffraction peaks indicates that the sizes of the TiO₂ or the NiS₂/TiO₂ particles are very small and the estimated particle sizes by Scherrer equation are *ca.* 15 nm. However, the strong (002) diffractions of the hexagonal graphite at 2 θ of about 25.88°, it is very difficult to discover it in all of the composites due to strong overlapping by the TiO₂ diffraction peak.

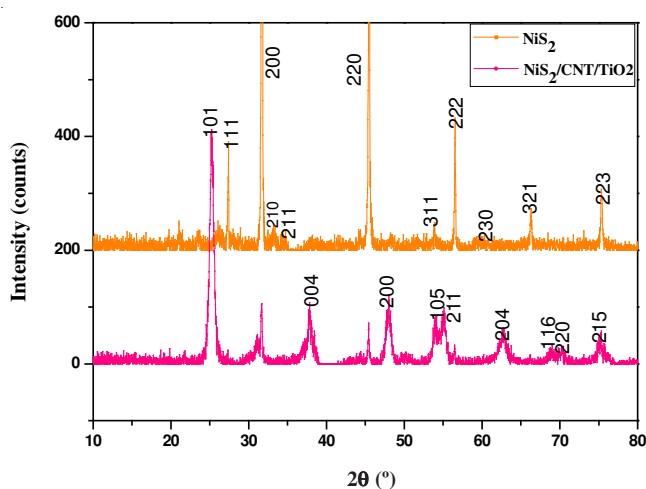


Fig. 2. XRD patterns of NiS₂ and NiS₂/CNT/TiO₂ composites

EDX was carried out to probe composition and element weight per cent of the attached nanoparticles. The spectrum is shown in Fig. 3 for NiS₂/TiO₂, CNTs/TiO₂ and NiS₂/TiO₂-

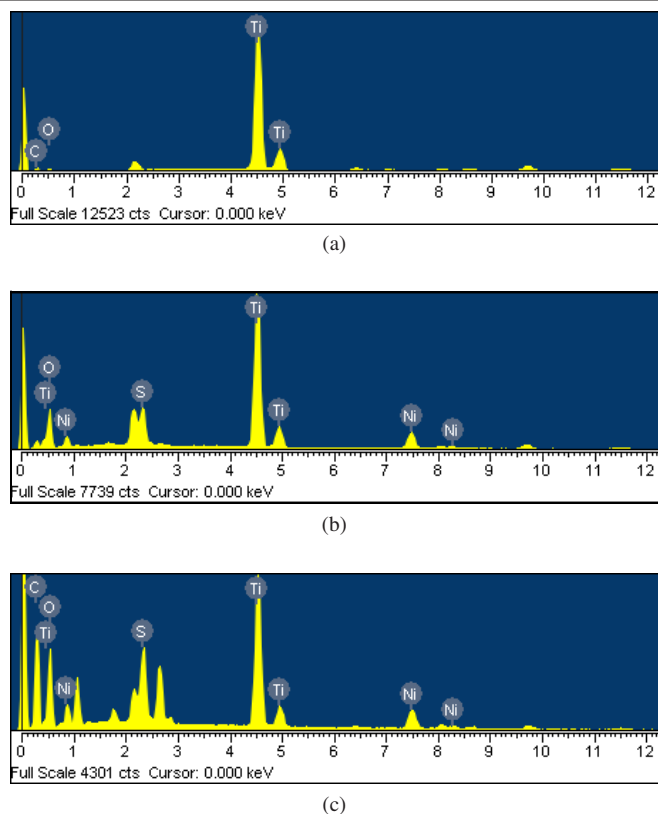


Fig. 3. EDX analysis of as-prepared composite: (a) CNT/TiO₂, (b) NiS₂/TiO₂, (c) NiS₂-CNTs/TiO₂-MWCNT

MWCNT composites. The data of EDX analyses of the as-prepared composites were listed in Table-2. The main elements as presence of strong Ti, O peaks of 4.51, 4.92 and 0.52 keV, separately were observed in TiO₂ and CNTs/TiO₂ composites. Meanwhile, a new element Ni and S were observed in NiS₂/TiO₂ and NiS₂-CNTs/TiO₂-MWCNT composites, which confirms not only the TiO₂ particles were existed, but NiS₂ was also existed.

The specific surface areas (BET) of the as-prepared composites were also listed in Table-2. In comparison with MWCNTs, The BET value was decreased from 211.43 m²/g of MWCNTs to 101.27 m²/g of CNT/TiO₂. The BET surface area was decreased to 52.37 m²/g when the NiS₂ particles were obtained in NiS₂-CNTs/TiO₂-MWCNT composites. This suggests that the TiO₂ and NiS₂ nanoparticles were introduced into the pores of the MWCNTs, which decreased the BET surface area. Compared with pure TiO₂, the surface area of NiS₂/TiO₂ photocatalysts was increased slightly. The reason might be that when the NiS₂ nanoparticles were distributed on the surface of TiO₂ thus formed a certain amount of mesopores and macropores.

TABLE-2
EDX ELEMENTAL MICROANALYSIS, BET SURFACE AREAS AND VISIBLE LIGHT
PHOTO-DEGRADATION RATE (k_{app}) CONSTANTS OF PHOTOCATALYSTS

Sample name	C (%)	O (%)	Ti (%)	Ni (%)	S (%)	Impurity (%)	BET (m ² /g)	k_{app} (min ⁻¹)
MWCNTs	99.99	—	—	—	—	0.01	211.43	—
TiO ₂	—	45.22	54.78	—	—	—	11.59	0
NiS ₂ /TiO ₂	—	57.17	24.69	15.42	2.72	—	60.39	1.28×10^{-3}
CNT/TiO ₂	20.84	44.11	35.05	—	—	—	101.27	1.23×10^{-3}
NiS ₂ -CNT/TiO ₂	15.69	43.14	27.08	10.88	3.21	—	52.37	2.66×10^{-3}

Visible light photocatalytic studies: The photodegradation studies in aqueous suspension containing TiO₂, NiS₂/TiO₂, CNT/TiO₂ and NiS₂-CNT/TiO₂ composite catalyst was shown in Fig. 4. The adsorption effect of CNT/TiO₂ on methyl orange was faster than that of any other photocatalysts. This was attributed to the high porosity of the CNT/TiO₂ surface due to introduction of MWCNTs, which correlated with an increase in adsorption ability. However, in the presence of CNT/TiO₂, degradation of methyl orange was observed but it shown a little low photocatalytic efficiency. It can be considered that when the particle size was small and appeared agglomeration after heat treatment the probability of electron-hole recombination was increased which results its photocatalytic efficiency was reduced. For NiS₂/TiO₂ samples, it exhibited a higher visible light photocatalytic activity than CNT/TiO₂. Among these samples, sample NiS₂-CNT/TiO₂ exhibited the highest visible light photocatalytic activity after irradiation for 150 min.

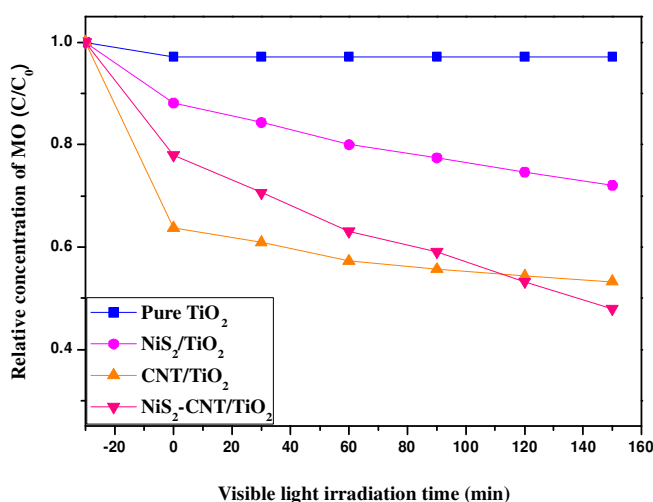


Fig. 4. Photocatalytic degradation behaviors of methyl orange for the as-prepared photocatalysts under visible light irradiation

Photocatalytic reactions with different photocatalysts can be expressed by the Langmuir-Hinshelwood model. The photocatalytic degradation of methyl orange containing different photocatalysts under visible light obeys pseudo-first-order kinetics with respect to the concentration of methyl orange:

$$-\frac{dc}{dt} = k_{app}C \quad (1)$$

Integration of this equation (with the restriction of $c = c_0$ at $t = 0$, with c_0 being the initial concentration in the bulk solution after dark adsorption and t the reaction time) will lead to the following expected relation:

$$-\ln\left(\frac{c_t}{c_0}\right) = k_{app}t \quad (2)$$

where c_t and c_0 are the reactant concentrations at times $t = t$ and $t = 0$, respectively and k_{app} and t are the apparent reaction rate constant and time, respectively. According to this equation, a plot of $-\ln(c_t/c_0)$ versus t will yield a slope of k_{app} . The results are displayed in Fig. 5 and also summarized in Table-2. The methyl orange degradation rate constant for NiS₂-CNT/TiO₂

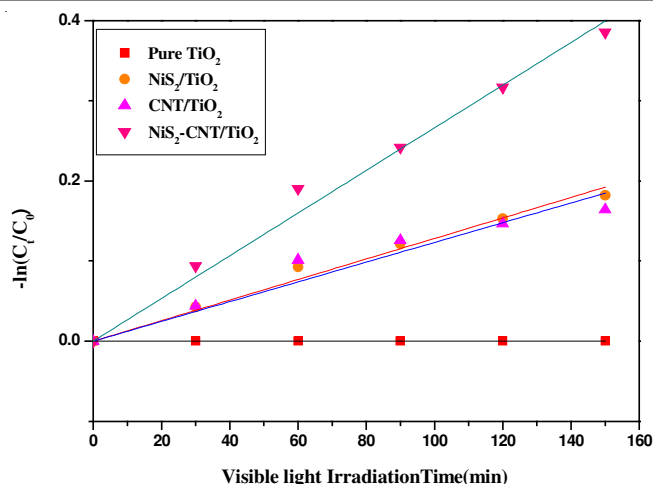


Fig. 5. Apparent first order kinetics of methyl orange degradation in presence of pure TiO₂, NiS₂/TiO₂, CNT/TiO₂ and NiS₂-CNT/TiO₂ photocatalysts under visible light irradiation

composites reaches $2.66 \times 10^{-3} \text{ min}^{-1}$ under visible light, both of which are much higher than the corresponding values for pure TiO₂, NiS₂/TiO₂ and CNT/TiO₂. The above results suggest that the NiS₂-CNT/TiO₂ composites are much more effective photocatalysts than any other composites. The excellent photocatalytic activity could be attributed to the synergistic effects of high charge mobility and MWCNTs may act as support, absorbent, photo-generated transfer station. Based on literature reports^{19,20} and our experiment results, we propose a mechanism for the degradation of pollutants on NiS₂ coupled TiO₂ catalyst under visible light irradiation as shown in Fig. 6. In the heterojunction composite, the generated electrons from NiS₂ may migrate freely to the conduction band (CB) of TiO₂ and then transfer to the surface of MWCNT and the photo induced holes on the TiO₂ surface migrate to NiS₂ owing to the different valence band edge potentials. In this way, the photo induced electron-hole pairs in the two semiconductors are effectively separated and the probability of electron-hole recombinations is reduced. In addition, the generated electrons probably react with dissolved oxygen molecules and produce oxygen peroxide radical $\text{O}_2^{\cdot-}$, the positive charged hole (h^+) may react with the OH^- derived from H_2O to form hydroxyl radical OH^{\cdot} . It is well known that the $\text{O}_2^{\cdot-}$ and OH^{\cdot} are powerful oxidizing agent capable of degrading most pollutants

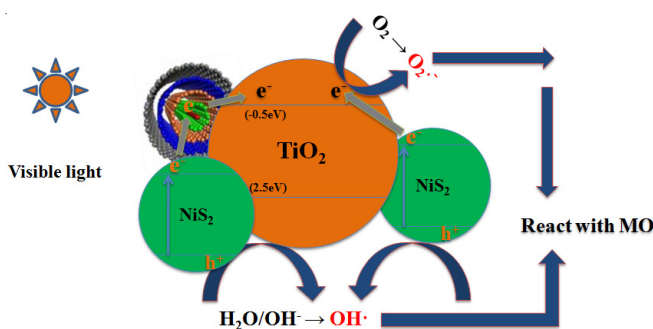


Fig. 6. Scheme of excitation and charge transfer process between NiS₂ and TiO₂ in the NiS₂-CNT/TiO₂ composite

Conclusion

This paper presents a sol-gel method for preparation of the efficient photocatalytic materials NiS₂-CNT/TiO₂ nanocomposites. The porous structure and the NiS₂ and TiO₂ particles coated on the surface of MWCNTs can be observed from SEM and TEM images analysis. The composites show efficient visible-light photocatalytic activity to degrade the aqueous methyl orange, which is higher than that of pure TiO₂ photocatalyst. This efficient photocatalytic activity is attributed to this indicates that the presence of the MWCNTs can not only efficiently inhibit the agglomeration of NiS₂/TiO₂ nanoparticles, but also improve the photocatalytic efficiency due to the recombination of e⁻/h⁺ pairs is retarded and the synergistic effect of semiconductor NiS₂.

REFERENCES

1. M. Romero, J. Blanco, B. Sanchez, A. Vidal, S. Malato, A.I. Cardona and E. Garcia, *Solar Energy*, **66**, 169 (1999).
2. M. Anpo and M. Takeuchi, *J. Catal.*, **216**, 505 (2003).
3. H. Irie, Y. Watanabe and K. Hashimoto, *J. Phys. Chem. B*, **107**, 5483 (2003).
4. H. Kisch, L. Zang, C. Lange, W.F. Maier, C. Antonis and D. Angew. Meissner, *Chem. Int. Ed.*, **37**, 3034 (1998).
5. H. Su, Y. Xie, P. Gao, Y. Xiong and Y. Qian, *J. Mater. Chem.*, **11**, 684 (2001).
6. P.G. Niklowitz, P.L. Alireza, M.J. Steiner, G.G. Lonzarich, D. Braithwaite, G. Knebel, J. Flouquet and J.A. Wilson, *Phys. Rev. B*, **77**, 115135 (2008).
7. A. Kongkanand and P.V. Kamat, *ACS Nano*, **1**, 13 (2007).
8. R.M. Paula, P. Kumbhakara and A.K. Mitra, *Sci. Eng. B*, **167**, 97 (2010).
9. A. Profumo, M. Fagnoni, D. Merli, E. Quartarone, S. Protti and D. Dondi, *Anal. Chem.*, **78**, 4194 (2006).
10. C. Lettmann, K. Hildenbrand, H. Kisch, W. Macyk and W.F. Maier, *Appl. Catal. B: Environ.*, **32**, 215 (2001).
11. S. Sakthivel and H. Angew. Kisch, *Chem. Int. Ed.*, **42**, 4908 (2003).
12. S.Y. Treschev, P.W. Chou, Y.H. Tseng, J.B. Wang, E.V. Perevedentseva and C.L. Cheng, *Appl. Catal. B: Environ.*, **79**, 8 (2008).
13. T. Ohno, M. Akiyoshi, T. Umebayashi, K. Asai, T. MitSui and M. Matsumura, *Appl. Catal. A: Gen.*, **265**, 115 (2004).
14. L. Lin, W. Lin, J.L. Xie, Y.X. Zhu, B.Y. Zhao and Y.C. Xie, *Appl. Catal. B: Environ.*, **75**, 52 (2007).
15. H. Luo, T. Takata, Y. Lee, J. Zhao, K. Domen and Y. Yan, *Chem. Mater.*, **16**, 846 (2004).
16. I. Kang, Q. Zhang, S. Yin, T. Sato and F. Saito, *Appl. Catal. B: Environ.*, **80**, 81 (2008).
17. G.S. Wu, T. Nishikaw, B. Ohtana and A.C. Chen, *Chem. Mater.*, **17**, 4530 (2007).
18. L.L. Wang, Y.C. Zhu, H.B. Li, Q.W. Li and Y.T. Qian, *J. Solid State Chem.*, **183**, 223 (2010).
19. H. Li, B. Zhu, Y. Feng, S. Wang, S. Zhang and W. Huang, *J. Solid State Chem.*, **180**, 2136 (2007).
20. Y. Xie, S.H. Heo, Y.N. Kim, S.H. Yoo and S.O. Cho, *Nanotechnology*, **21**, 015702 (2010).